Nanodiamond Nanofluids for Enhanced Thermal Conductivity

Blake T. Branson,[†] Paul S. Beauchamp,[‡] Jeremiah C. Beam,[§] Charles M. Lukehart,[§,*] and Jim L. Davidson[⊥,*]

[†]Interdisciplinary Materials Science, [‡]Department of Mechanical Engineering, [§]Department of Chemistry, and [⊥]Department of Electrical Engineering, Vanderbilt University, Nashville, Tennessee 37235, United States

ABSTRACT Deaggregation of oxidized ultradispersed diamond (UDD) in dimethylsulfoxide followed by reaction with glycidol monomer, purification *via* aqueous dialysis, and dispersion in ethylene glycol (EG) base fluid affords nanodiamond (ND)—poly(glycidol) polymer brush:EG nanofluids exhibiting 12% thermal conductivity enhancement at a ND loading of 0.9 vol %. Deaggregation of UDD in the presence of oleic acid/octane followed by dispersion in light mineral oil and evaporative removal of octane gives ND·oleic acid:mineral oil dispersions exhibiting 11% thermal conductivity enhancement at a ND loading of 1.9 vol %. Average particle sizes of ND additives, determined by dynamic light scattering, are, respectively, *ca.* 11 nm (in H_2O) and 18 nm (in toluene). Observed thermal conductivity enhancements outperform enhancement effects calculated using Maxwell's effective medium approximation by 2- to 4-fold. Covalent ND surface modification gives 2-fold greater thermal conductivity enhancement than ND surface modification *via* hydrogen-bonding interactions at similar concentrations. Stable, static ND:mineral oil dispersions are reported for the first time.

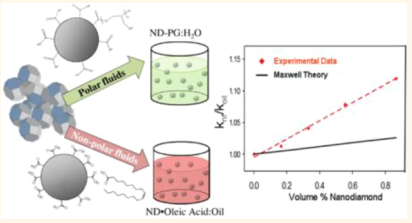

KEYWORDS: nanodiamond · nanofluid · thermal conductivity · surface functionalization · surfactant

Heat-transfer fluids, such as water, mineral oil, and ethylene glycol, serve important functions in many thermal transport applications but suffer from low thermal conductivity. Efficiencies of fluid thermal systems would be enhanced substantially if higher thermal conductivities of working fluids can be achieved. Incorporation of small solid materials of high thermal conductivity into base liquids was shown by Maxwell to improve thermal conductivity of base liquids.[1] Adding micrometer-sized particles to a fluid, however, presents several drawbacks including increased pumping power requirements, enhanced clogging of narrow channels, possible erosion of pipe walls, and rapid settling of additive particles.

Dispersion of nanometer-sized solid materials in base fluids, classified as "nanofluids" by Choi in 1995,[2] has attracted much recent interest. Addition of less than 1 vol % of nanoparticle material to base fluids can lead to double-digit percentage enhancements of thermal conductivity.[3] However, others have reported observing no anomalous nanofluid enhancement effects.[4] As an emerging field of study, both the magnitude of nanofluid thermal conductivity enhancements and mechanisms responsible for such effects continue to be topics of debate. Participating factors include Brownian motion, radiative heat transfer, interfacial layering, and effect of particle aggregation.[5,6] Jang *et al.* have attempted to develop a theory to explain the unexpected performance of nanoparticles by accounting for the four factors that determine the thermal conductivity of a nanofluid: collisions between the base fluid molecules, interfacial thermal resistance, Brownian motion of the nanoparticles, and an additional term that accounts for the dynamic interactions between the nanoparticles and the base fluid.[7] Nanoparticles, constantly moving due to Brownian motion, rapidly and repeatedly interact with the surrounding fluid molecules. These nanoscale collisions represent a mode of thermal energy transfer not present at larger scales. Macroscopically, this phenomenon manifests itself as conduction because net movement of particles under Brownian motion is zero.

Ideally, nanoparticulate additives must be well dispersed and stable in the desired base fluid. Specialized processing techniques, such as surface hydrogenation[8] or use of surfactants, are usually required to achieve high-quality colloidal dispersions.

Low-aspect ratio nanomaterials including metals (copper,[9] silver,[10] and gold[6])

* Address correspondence to charles.m.lukehart@vanderbilt.edu.

Received for review December 7, 2012 and accepted March 14, 2013.

Published online March 14, 2013
10.1021/nn305664x

and metal oxides (copper oxide,[11] alumina,[12] and titania[10]) have been used as nanofluid additives. Diamond is a nanofluid additive of particular interest due to its very high thermal conductivity, high hardness, relatively low density, and very low electrical conductivity. Ultradispersed diamond (UDD) powder,[13] a commercial source of nanodiamond, consists of 0.1−2 μm aggregates of nanodiamond crystallites (diameters <10 nm) embedded within a fullerene carbon matrix. When UDD is dispersed in ethylene glycol (EG) or various oils, little enhancement of base fluid thermal conductivity is observed due to its very poor dispersibility.[14−17] Methods for deaggregating UDD powder permit isolation of the primary nanodiamond (ND) crystallites on a commercial scale; however, achieving stable ND/base fluid dispersions usually requires ND surface modification *via* gas annealing techniques[18] or the addition of surfactant-based or covalently bound functional groups.

Highly aggregated ND:Syltherm 800 [a commercial poly(dimethylsiloxane) fluid] dispersions show no significant enhancement in thermal conductivity up to 3.5 vol % ND loading.[19] Thermal conductivity enhancements have been observed to various degrees for ND dispersions in base fluids containing OH groups, such as water, EG, EG/water, or Midel oil.[15,20−25] Stable dispersions are most commonly achieved using surface-oxidized ND with pH adjustment. At 30 °C, thermal conductivity enhancements of 7.2% and 17.2% have been reported, respectively, for ND:water (3 vol % ND loading)[21] and ND:EG (1 vol % ND loading)[20] static dispersions. Achieving stable ND:mineral oil dispersions remains a critical challenge relevant to cooling transformer oils or other nonpolar fluids.

We now report successful preparations of stable, static ND:EG and ND:mineral oil dispersions having maximum ND loadings of 0.9−1.9 vol %, respectively, and high thermal conductivity enhancements. Dispersions in EG are achieved with covalent surface modification *via* formation of ND−poly(glycidol) polymer brushes, while dispersions in light mineral oil are achieved using oleic acid as a surfactant. Formation of stable, static ND:mineral oil dispersions has now been achieved for the first time.

RESULTS AND DISSCUSSION

ND−Poly(glycidol) Polymer Brush:EG Nanofluids. Synthesis strategies for obtaining stable, static nanodiamond:base fluid dispersions commonly require deaggregation of a nanodiamond source, such as UDD powder, followed by diamond surface modification to enhance solvation.[17] Ultrasonic dispersion of air-oxidized UDD powder (ox-UDD) in dimethylsulfoxide (DMSO) liquid gives ox-UDD:DMSO dispersions containing highly aggregated nanodiamond particulates (0.05 μm to >1 μm diameter) (Figure 1a). However, bead-milling ox-UDD in DMSO liquid produces efficient deaggregation, resulting in ND:DMSO dispersions having

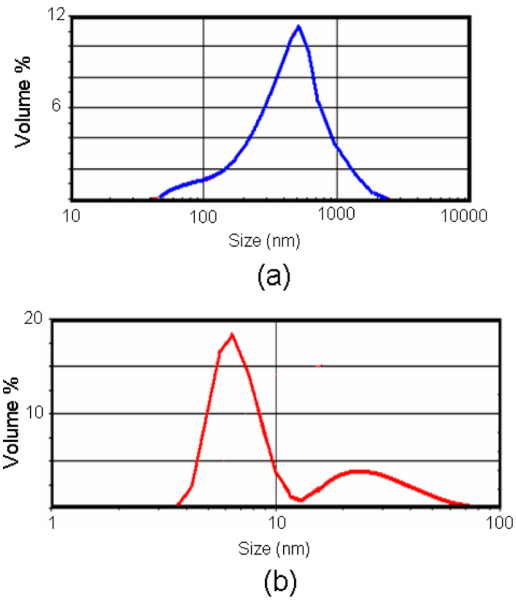

Figure 1. Particle size distributions for (a) ox-UDD:DMSO and (b) deaggregated ND:DMSO dispersions, as determined by dynamic light scattering (DLS).

bimodal particle-size distribution (Figure 1b) with an average particle size of ca. 8 nm, consistent with the size of primary nanodiamond crystallites found within UDD powder.[18,26,27]

Stable, static ND:ethylene glycol (ND:EG) dispersions are achieved when ND particles are surface-modified by poly(glycidol) polymer brushes. Treating ND:DMSO dispersions with glycidol at elevated temperature permits covalent condensation of glycidol monomers with ND-COOH surface groups followed by ring-opening glycidol oligomerization to give ND−poly(glycidol) polymer brush:DMSO dispersions (Figure 2; top).[18] Purification and solvent exchange *via* aqueous dialysis gives an intermediate ND−poly(glycidol) polymer brush:H_2O dispersion that, upon solvent exchange with EG, gives a final stable, static ND−poly(glycidol) polymer brush:EG dispersion. Dynamic light scattering (DLS) particle-size distributions of the intermediate aqueous dispersion (Figure 2; bottom) reveal an increase in average ND particle size to *ca.* 11 nm, consistent with solvation of ND particles now containing poly(glycidol) polymer brush chains as surface modification. ND flocculation is inhibited by strong solvation of hydroxyl groups present within these polymer brush chains.[27]

Thermogravimetric analysis (TGA) of an aliquot of ND−poly(glycidol) polymer brush:H_2O dispersion reveals evaporative loss of water at T < 100 °C and a second mass-loss event centered at *ca.* 350 °C ascribed to thermal degradation of covalently bound poly(glycidol) chains leaving a ND residue (see Figure 3). Loss of mass due to the presence of free glycidol (bp = 167 °C) is not observed. FTIR spectral data of ND−poly(glycidol) material (Figure S1) reveal a C═O

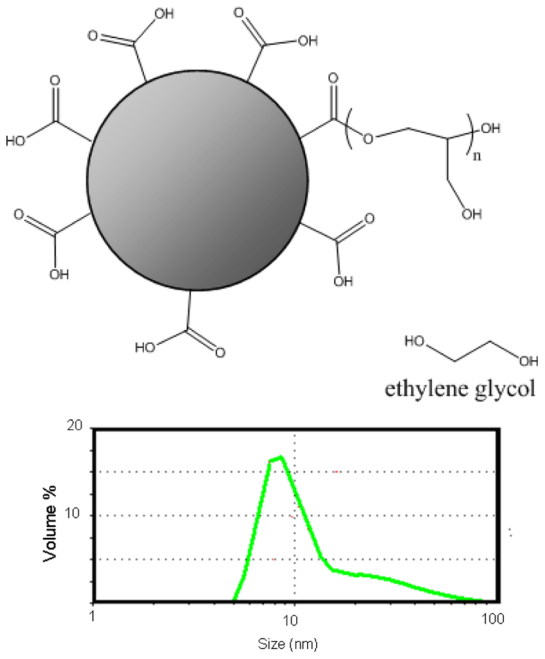

Figure 2. (top) Cartoon depiction of a ND−poly(glycidol) polymer brush nanoparticle and EG. (bottom) DLS particle-size distribution of a ND-poly(glycidol) polymer brush dispersion in water.

stretching band at *ca.* 1733 cm^{-1}, consistent with covalent binding of poly(glycidol) polymer brush chains to ND surface sites through ester functional groups (as depicted in Figure 2) and absence of a C═O stretching band near 1776 cm^{-1} expected of surface COOH/anhydride groups. Each gram of nanodiamond contains *ca.* 3 g of surface-bound oligomer. Acid−base titration[28] of ND−COOH powder reveals a reactive COOH content of 4.8 mmol of COOH/g. Assuming that each surface COOH functional group is used for glycidol oligomerization, the calculated average glycidol polymer brush chain length is *ca.* 9-mer. Energy dispersive spectral data (Figure S2) of dried ND−poly(glycidol) polymer brush material reveal a Zr content of <1 at. % due to residual contamination from bead-milling. This level of contamination represents a negligible Zr contamination of *ca.* 0.01 vol % for nanofluids tested for thermal conductivity.

ND·Oleic Acid:Mineral Oil Nanofluids. Formation of stable, static ND:mineral oil base fluid dispersions requires nonpolar ND surface modification.[29,30] Deaggregation of UDD powder in the presence of oleic acid and octane gives a transparent dark red dispersion. Addition of light mineral oil and evaporative removal of octane affords ND−oleic acid/mineral oil dispersions having a deep brown color characteristic of deaggregated nanodiamond solutions (Figure 4).[31] At narrow path length, these dispersions appear red, indicative of Rayleigh scattering from particles much smaller than the wavelength of visible light (Figure 5). DLS particle-size distributions of ND·oleic acid dispersions in toluene are monomodal, showing an average particle size of *ca.*

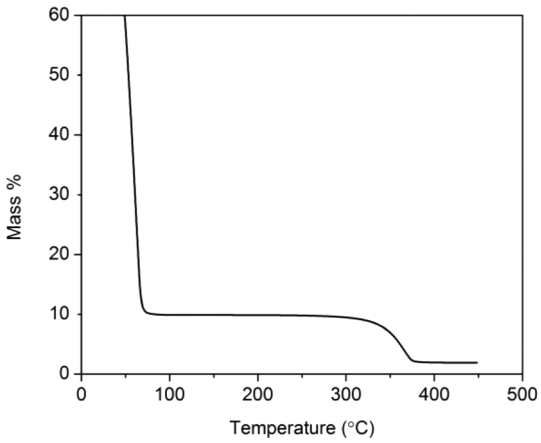

Figure 3. TGA trace of mass loss of an aliquot of ND−poly(glycidol):H_2O nanofluid dispersion.

Figure 4. Photograph of a ND·oleic acid:mineral oil dispersion. Transparent section on the right has 1 mm thickness.

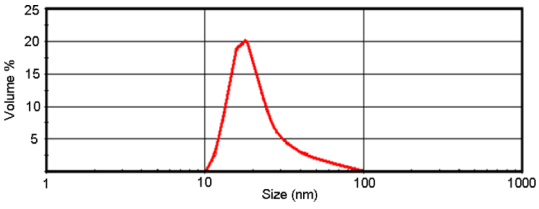

Figure 5. DLS particle-size distribution measured for a ND·oleic acid:toluene dispersion.

18 nm (Figure 5), consistent with long-chain hydrocarbon surface passivation.

Mass-loss analysis of an aliquot of ND·oleic acid:octane dispersion reveals evaporative loss of octane base fluid at $T < 120$ °C and continuous mass loss over the range 150−500 °C (Figure 6), probably due to evaporative loss of free oleic acid (bp = 360 °C) as well as evaporation loss/thermal degradation of oleic acid involved in hydrogen bonding to ND−COOH surface groups.[32] Approximately half of this second mass loss occurs at $T > 360$ °C.

To enhance formation of ND−COOH·oleic acid hydrogen bonding yet minimize oleic acid bilayer formation, only enough oleic acid is used in the initial

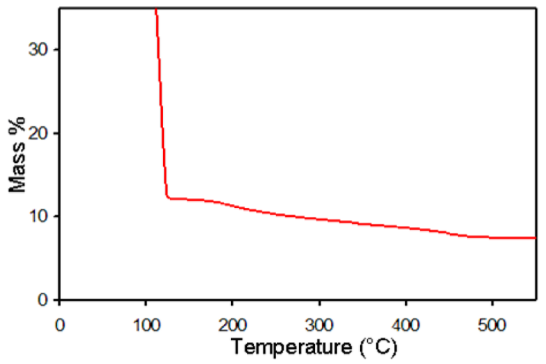

Figure 6. TGA trace of ND·oleic acid:octane nanofluid.

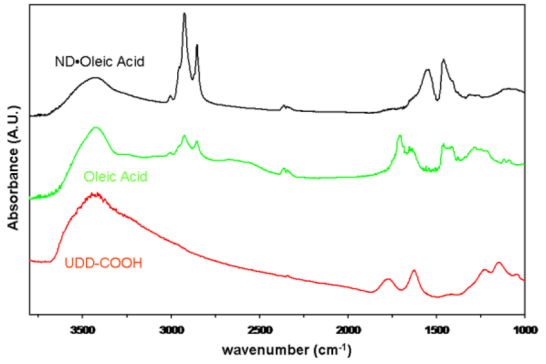

Figure 7. FT-IR spectra of ox-UDD, oleic acid, and ND·oleic acid powder.

ND·oleic acid:octane nanofluid synthesis to bind to *ca.* 70% of ND surface COOH groups. Comparison of Fourier-transform infrared (FT-IR) spectra of precipitated ND·oleic acid powder with those of oleic acid and ox-UDD shows all expected high-frequency bands for common functional groups (Figure 7).[33−35] However, the carboxyl C−O stretching band present at 1710 cm^{-1} in oleic acid is shifted to 1560 cm^{-1} in ND·oleic acid powder, consistent with essentially complete chemisorption of oleic acid head groups to ND−COOH surface sites.[36,37]

Strong association of oleic acid surfactant to ND surface sites is also supported by proton NMR spectroscopy. Comparison of ^{1}H NMR spectra of free oleic acid and ND·oleic acid dispersion in deuterated benzene reveals resonances at 1.03, 1.46, 2.31, and 5.69 ppm assigned to the expected terminal methyl (CH^d_3), methylene ($CH^{b,c}_2$), and vinylic (CH^a) hydrogen environments (Figure 8). However, extreme peak broadening observed in the ND·oleic acid resonances is diagnostic of reduced T_1 relaxation rates for proton resonances associated with chemisorbed molecules.[37]

Thermal Conductivity of ND−Poly(glycidol) Polymer Brush:EG and ND·Oleic Acid:Mineral Oil Nanofluids. Plots of thermal conductivity enhancement ratios (measured by the single hot-wire probe method) of ND−poly(glycidol) polymer brush:EG and ND·oleic acid:mineral oil nanofluids are shown in Figure 9 as a function of ND additive loading. The temperature dependence of thermal

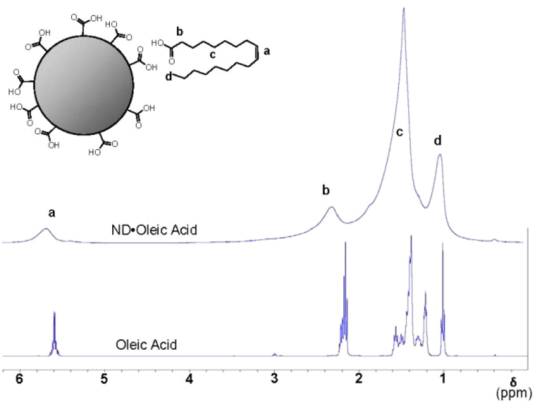

Figure 8. Comparison of ^{1}H NMR spectra of free oleic acid and ND·oleic acid in deuterated benzene.

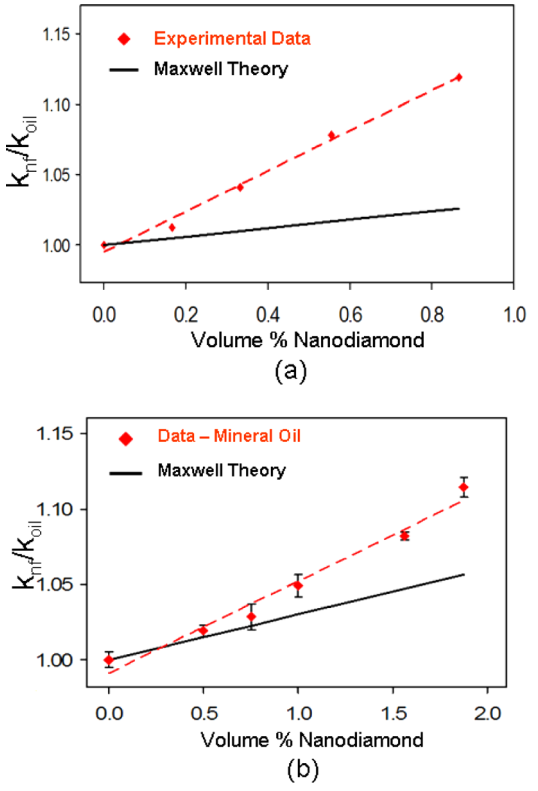

Figure 9. Thermal conductivity enhancement as a function of nanodiamond loading for (a) ND−poly(glycidol) polymer brush:ethylene glycol nanofluids and (b) ND·oleic acid: mineral oil nanofluids.

conductivity enhancement for ND·oleic acid:mineral oil nanofluids at several ND additive loadings is also provided (see Figure 10).

Incorporation of ND additives into either polar (EG) or nonpolar (mineral oil) base fluids enhances thermal conductivity. In EG, addition of 0.88 vol % ND additive gives 12% enhancement in thermal conductivity. In mineral oil, an enhancement of 11% is achieved at a ND additive loading of 1.9 vol %. The thermal conductivity enhancement ratio of ND·oleic acid:mineral oil nanofluids is temperature independent within experimental precision.

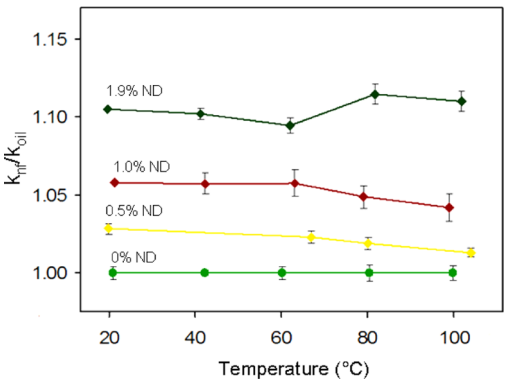

Figure 10. Temperature dependence of thermal conductivity enhancement ratio of ND·oleic acid:mineral oil nanofluids at ND additive loadings of 0, 0.5, 1.0, and 1.9 vol %.

Thermal conductivity enhancement ratios shown in Figure 9, derived from Maxwell's effective medium theory,[1] are calculated using the equation below:

$$\frac{k_{nf}}{k_f} = \frac{k_p + 2k_f - 2\varphi(k_f - k_p)}{k_p + 2k_f + \varphi(k_f - k_p)}$$

where k_{nf}, k_f, and k_p refer to the thermal conductivities of nanofluid, unfilled fluid, and the nanoparticle material, respectively, at a volume fraction φ. The thermal conductivity of diamond is several orders of magnitude greater than that of EG or mineral oil base fluids.[38] In such cases, $k_p \gg k_f$, and the above equation reduces to

$$\frac{k_{nf}}{k_f} = 1 + 3\varphi$$

As revealed in Figure 9, plots of experimental enhancement ratios deviate linearly from predicted values as

$$\frac{k_{nf}}{k_f} \approx 1 + 14\varphi$$

for ND−poly(glycidol) polymer brush:EG nanofluids and as

$$\frac{k_{nf}}{k_f} \approx 1 + 6\varphi$$

for ND·oleic acid:mineral oil nanofluids.

Although substantial deviation from Maxwell's theory is observed for ND−poly(glycidol) polymer brush:EG nanofluids, similar results have been recently reported for ND/EG dispersions at basic pH.[20] Previous studies of aggregated nanodiamond dispersions in nonpolar fluids have shown qualitative enhancement of thermal conductivity but have not provided quantitative values.[16,17] Enhancement ratios of ND·oleic acid:mineral oil nanofluids reported here are similar to enhancement ratio values observed for copper-filled nanofluids.[9]

Thermal conductivity enhancements at similar additive loading are more pronounced for ND−poly(glycidol) polymer brush:EG nanofluids than for ND·oleic acid:mineral oil nanofluids by more than a factor of 2. Both nanofluid systems use ND additive but with different modes of surface modification. Covalent surface functionalization is expected at the ND/polymer brush interface of ND:EG nanofluids, while noncovalent, hydrogen-bonding interactions are evident at the ND/surfactant interface of ND:mineral oil nanofluids. Differences in enhancement efficiencies are likely attributable to differences in thermal boundary resistance at nanoparticle/surfactant interfaces. Since thermal resistance at nanoparticle/organic interfaces is reduced by stronger coupling between these two phases,[39] covalently bound surface modifications are expected to give greater thermal conductivity enhancements than that from only van der Waals surface binding.

Although the role of Brownian motion in nanofluid thermal conductivity enhancement is debated,[7,40] it may be an important factor when the viscosity of a base fluid changes significantly with temperature,[41] which is certainly the case for mineral oils. When Brownian motion effects are important, nanofluid thermal conductivity enhancement increases with increasing temperature. The observed temperature independence of thermal conductivity enhancement for ND·oleic acid:mineral oil nanofluid (Figure 10) suggests only nominal contribution by Brownian motion.

CONCLUSIONS

Covalent surface modification of deaggregated ND particles *via* formation of poly(glycidol) polymer brush chains gives stable, static ND nanofluids in EG base fluid up to additive loadings of 1.9 vol %. Noncovalent surface modification of deaggregated ND particles by oleic acid at partial stoichiometric coverage forms stable, static ND nanofluids in light mineral oil base fluid up to additive loadings of 0.9 vol %. The thermal conductivity of both base fluids is enhanced by 11−12%. Nanofluid thermal conductivity enhancements outperform enhancements calculated using Maxwell's effective medium approximation. At similar ND loadings, greater thermal conductivity enhancement is achieved when using covalent surface modification. By designing ND covalent surface modifications that optimize ND/base fluid solvation, even greater enhancements of base fluid thermal conductivity are expected.

EXPERIMENTAL SECTION

General Methods. Ultradispersed diamond was obtained from Alit Corp (Kiev, Ukraine) and heated for 2 h in a 415 °C tube furnace under flowing air to enhance carboxylic acid/anhydride functionalities (ox-UDD).[35,42] Deaggregation of UDD or ox-UDD to give nanodiamond dispersions was accomplished using previously reported methods.[42] Glycidol, dimethyl sulfoxide, oleic acid, and octane were purchased from Sigma Aldrich (St. Louis, MO) and used as received. Ethylene glycol and light mineral oil were purchased from Fisher Scientific (Pittsburgh, PA) and used as received.

Ox-UDD was dispersed in the chosen solvent by ultrasonic bath using a Branson 3510 benchtop sonicator. Particle size

analysis was performed using a Malvern Instruments Zetasizer model ZS. Surface functionalization of the nanodiamond was determined by thermogravimetric analysis using a TA Instruments 2950 thermogravimetric analyzer under N_2 with a heating rate of 10 °C min^{-1} and by Fourier transform infrared spectroscopy on a Thermo Mattson Satellite FT-IR with samples prepared as KBr pellets. Nuclear magnetic resonance spectroscopy was performed with a Bruker NMR spectrometer operating at 400 MHz. Samples were dispersed in deuterated benzene. Thermal conductivity measurements were performed with a Decagon Devices KD2 Pro, which was calibrated against a sample of glycerol with known thermal conductivity. The single hot-wire probe was immersed in 150 mL of sample with at least 2.5 cm of separation between the probe and sample container; samples were placed inside a laboratory oven to ensure an isolated and stable thermal environment. For each concentration and temperature data point, at least 10 measurements were recorded with an hour between each test to ensure the sample was at thermal equilibrium.

Control specimens received the same processing treatment as the nanofluid samples; the carrier solvent was added to the base fluid then evaporated out at reduced pressure in a rotary evaporator with a water bath set at 80 °C. This step was included in order to remove any affect that residual solvent could have on both viscosity and thermal conductivity.

Preparation of ND:Ethylene Glycol Nanofluids. A 200 mL flask was charged with 2.0 g of oxidized UDD and 48.0 g of DMSO. The gray solution was placed in an ultrasonic bath for 30 min, then subjected to a deaggregation treatment until the UDD aggregates had been broken down to primary ND particles.[27,42,43] The ND:DMSO solution was placed in a 200 mL flask with 50 mL of glycidol and a magnetic stir bar, then sealed with a rubber septum. The flask was placed in a 50 °C oil bath, and the solution was stirred vigorously under N_2 for 24 h. The solution was removed from the bath, allowed to cool to room temperature, then placed in a dialysis bag immersed in deionized water. The water wash was changed every 12 h for four days to remove unbound glycidol monomer and solvent.

The ND−glycidol:H_2O dispersion was combined with an appropriate amount of ethylene glycol and placed in an ultrasonic bath for 20 min. The solution was then placed in a rotary evaporator under reduced pressure and elevated temperature until it was observed that liquid condensation ceased.

Preparation of ND:Mineral Oil Nanofluids. A 200 mL round-bottom flask was charged with 2.0 g of UDD, 2.0 g of oleic acid, and 63 g of octane. The light gray solution was placed in an ultrasonic bath for 1 h. The solution was then subjected to a deaggregation treatment.[42] This solution of deaggregated nanodiamond, now black but transparent, was combined with an appropriate amount of mineral oil and sonicated for an additional 1 h. The solution was placed in a rotary evaporator with an 80 °C water bath and approximately 725 mmHg pressure until liquid condensation ceased.

Conflict of Interest: The authors declare no competing financial interest.

Acknowledgment. Financial support from NSF IGERT grant 0333392 and U.S. Army contract W911-NF-04-2-0023 is gratefully acknowledged.

Supporting Information Available: Details of surface COOH titration, FTIR and EDS spectral analysis of ND−poly(glycidol) polymer brush, and deaggregation procedure for preparing ND−COOH:DMSO material. This material is available free of charge *via* the Internet at http://pubs.acs.org.

REFERENCES AND NOTES

1. Maxwell, J. C. *A Treatise on Electricity and Magnetism*, 2nd ed.; Clarendon Press: Oxford, 1881.
2. Choi, S. U. S. Nanofluids: From Vision to Reality Through Research. *J. Heat Transfer* **2009**, *131*, 033106/1–033106/9.
3. Eastman, J. A.; Choi, S. U. S.; Li, S.; Yu, W.; Thompson, L. J. Anomalously Increased Effective Thermal Conductivities of Ethylene Glycol-Based Nanofluids Containing Copper Nanoparticles. *Appl. Phys. Lett.* **2001**, *78*, 718–720.
4. Putnam, S. A.; Cahill, D. G.; Braun, P. V.; Ge, Z.; Shimmin, R. G. Thermal Conductivity of Nanoparticle Suspensions. *J. Appl. Phys.* **2006**, *99*, 084308/1–084308/6.
5. Murshed, S. M. S.; Leong, K. C.; Yang, C. A Combined Model for the Effective Thermal Conductivity of Nanofluids. *Appl. Therm. Eng.* **2009**, *29*, 2477–2483.
6. Wen, D.; Lin, G.; Vafaei, S.; Zhang, K. Review of Nanofluids for Heat Transfer Applications. *Particuology* **2009**, *7*, 141–150.
7. Jang, S. P.; Choi, S. U. S. Role of Brownian Motion in the Enhanced Thermal Conductivity of Nanofluids. *Appl. Phys. Lett.* **2004**, *84*, 4316–4318.
8. Williams, O. A.; Hees, J.; Dieker, C.; Jager, W.; Kirste, L.; Nebel, C. E. Size-Dependent Reactivity of Diamond Nanoparticles. *ACS Nano* **2010**, *4*, 4824–4830.
9. Garg, J.; Poudel, B.; Chiesa, M.; Gordon, J. B.; Ma, J. J.; Wang, J. B.; Ren, Z. F.; Kang, Y. T.; Ohtani, H.; Nanda, J.; *et al.* Enhanced Thermal Conductivity and Viscosity of Copper Nanoparticles in Ethylene Glycol Nanofluid. *J. Appl. Phys.* **2008**, *103*, 074301/1–074301/6.
10. Lotfi, H.; Shafii, M. B. Boiling Heat Transfer on a High Temperature Silver Sphere in Nanofluid. *Int. J. Therm. Sci.* **2009**, *48*, 2215–2220.
11. Vajjha, R. S.; Das, D. K. Experimental Determination of Thermal Conductivity of Three Nanofluids and Development of New Correlations. *Int. J. Heat Mass Transfer* **2009**, *52*, 4675–4682.
12. Ju, Y. S.; Kim, J.; Hung, M. T. Experimental Study of Heat Conduction in Aqueous Suspensions of Aluminum Oxide Nanoparticles. *J. Heat Transfer* **2008**, *139*, 092403/1–092403/6.
13. Dolmatov, V. Y. Detonation Synthesis Ultradispersed Diamonds: Properties and Applications. *Russ. Chem. Rev.* **2001**, *70*, 607–626.
14. Torii, S.; Yang, W.-J. Heat Transfer Augmentation of Aqueous Suspensions of Nanodiamonds in Turbulent Pipe Flow. *J. Heat Transfer* **2009**, *131*, 043203/1–043203/5.
15. Xie, H.; Yu, W.; Li, Y. Thermal Performance Enhancement in Nanofluids Containing Diamond Nanoparticles. *J. Phys. D: Appl. Phys.* **2009**, *42*, 095413/1–095413/5.
16. Davidson, J. L.; Kang, W. P. Applying CVD Diamond and Particulate Nanodiamond. In *Synthesis, Properties and Applications of Ultrananocrystalline Diamond*; Gruen, D. M.; Shenderova, O. A.; Vul', A. Y., Eds.; Springer: New York, 2005; Vol. NATO Science Series II: Mathematics, Physics, and Chemistry; pp 357−373.
17. Tyler, T.; Shenderova, O.; Cunningham, G.; Walsh, J.; Drobnik, J.; McGuire, G. Thermal Transport Properties of Diamond-Based Nanofluids and Nanocomposites. *Diamond Relat. Mater.* **2006**, *15*, 2078–2081.
18. Zhao, L.; Takimoto, T.; Ito, M.; Kitagawa, N.; Kimura, T.; Komatsu, N. Chromatographic Separation of Highly Soluble Diamond Nanoparticles Prepared by Polyglygerol Grafting. *Angew. Chem., Int. Ed.* **2011**, *50*, 1388–1392.
19. Yang, Y.; Oztekin, A.; Neti, S.; Mohapatra, S. Particle Agglomeration and Properties of Nanofluids. *J. Nanopart. Res.* **2012**, *14*, 852/1–852/10.
20. Yu, W.; Xie, H.; Li, Y.; Chen, L.; Wang, Q. Experimental Investigation on the Thermal Transport Properties of Ethylene Glycol Based Nanofluids Containing Low Volume Concentration Diamond Nanoparticles. *Colloids Surf., A* **2011**, *380*, 1–5.
21. Yeganeh, M.; Shahtahmasebi, N.; Kompany, A.; Goharshadi, E. K.; Youssefi, A.; Siller, L. Volume Fraction and Temperature Variations of the Effective Thermal Conductivity of Nanodiamond Fluids in Deionized Water. *Int. J. Heat Mass Transfer* **2010**, *53*, 3186–3192.
22. Torii, S.; Yang, W.-J. Heat Transfer Augmentation of Aqueous Suspensions of Nanodiamonds in Turbulent Pipe Flow. *J. Heat Transfer* **2009**, *131*, 043203/1–043203/5.
23. Tyler, T.; Shenderova, O.; Cunningham, G.; Walsh, J.; Drobnik, J.; McGuire, G. Thermal Transport Properties of Diamond-Based Nanofluids and Nanocomposites. *Diamond Relat. Mater.* **2006**, *15*, 2078–2081.
24. Ma, H. B.; Wilsom, C.; Borgmeyer, B.; Park, K.; Yu, Q.; Choi, S. U. S.; Tirumala, M. Effect of Nanofluid on the Heat

Transport Capability in an Oscillating Heat Pipe. *Appl. Phys. Lett.* **2006**, *88*, 143116/1–143116/3.
25. Ding, Y.; Chen, H.; He, Y.; Lapkin, A.; Yeganeh, M.; Siller, L.; Butenko, Y. V. Forced Convective Heat Transfer of Nanofluids. *Adv. Powder Technol.* **2007**, *18*, 813–824.
26. Shenderova, O. A.; Zhirnov, V. V.; Brenner, D. W. Carbon Nanostructures. *Crit. Rev. Sol. State Mater. Sci.* **2002**, *27*, 227–356.
27. Ozawa, M.; Inaguma, M.; Takahashi, M.; Kataoka, F.; Krüger, A. E.; Osawa, E. Preparation and Behavior of Brownish, Clear Nanodiamond Colloids. *Adv. Mater.* **2007**, *19*, 1201–1206.
28. Schmidlin, L.; Pichot, V.; Comet, M.; Josset, S.; Rabu, P.; Spitzer, D. Identification, Quantification and Modification of Detonation Nanodiamond Functional Groups. *Diamond Relat. Mater.* **2012**, *22*, 113–117.
29. Krueger, A. The Structure and Reactivity of Nanoscale Diamond. *J. Mater. Chem.* **2008**, *18*, 1485–1492.
30. Mochalin, V. N.; Gogotsi, Y. Wet Chemistry Route to Hydrophobic Blue Fluorescent Nanodiamond. *J. Am. Chem. Soc.* **2009**, *131*, 4594–4595.
31. Eidelman, E. D.; Siklitsky, V. I.; Sharanova, L. V.; Yagovkina, M. A.; Vul', A. Y.; Takahashi, M.; Inakuma, M.; Ozawa, M.; Osawa, E. A Stable Suspension of Single Ultrananocrystalline Diamond Particles. *Diamond Relat. Mater.* **2005**, *14*, 1765–1769.
32. Rosen, M. J. *Surfactants and Interfacial Phenomena*, 3rd ed.; John Wiley & Sons: Hoboken, NJ, 2004; p 444.
33. Liang, Y.; Ozawa, M.; Krueger, A. A General Procedure to Functionalize Agglomerating Nanoparticles Demonstrated on Nanodiamond. *ACS Nano* **2009**, *3*, 2288–2296.
34. Jiang, T.; Xu, K. FTIR Study of Ultradispersed Diamond Powder Synthesized by Explosive Detonation. *Carbon* **1995**, *33*, 1663–1671.
35. Osswald, S.; Yushin, G.; Mochalin, V.; Kucheyev, S. O.; Gogotsi, Y. Control of sp^2/sp^3 Carbon Ratio and Surface Chemistry of Nanodiamond Powders by Selective Oxidation in Air. *J. Am. Chem. Soc.* **2006**, *128*, 11635–11642.
36. Zhang, L.; He, R.; Gu, H.-C. Oleic Acid Coating on the Monodisperse Magnetite Nanoparticles. *Appl. Surf. Sci.* **2006**, *253*, 2611–2617.
37. Li, L.; Davidson, J. L.; Lukehart, C. M. Surface Functionalization of Nanodiamond Particles *via* Atom Transfer Radical Polymerization. *Carbon* **2006**, *44*, 2308–2315.
38. Kakac, S.; Pramuanjaroenkij, A. Review of Convective Heat Transfer Enhancement with Nanofluids. *Int. J. Heat Mass Transfer* **2009**, *52*, 3187–3196.
39. Shenogin, S.; Xue, L. P.; Ozisik, R.; Keblinski, P.; Cahill, D. G. Role of Thermal Boundary Resistance on the Heat Flow in Carbon-Nanotube Composites. *J. Appl. Phys.* **2004**, *95*, 8136–8144.
40. Li, C. H.; Peterson, G. P. Mixing Effect on the Enhancement of the Effective Thermal Conductivity of Nanoparticle Suspensions (Nanofluids). *Int. J. Heat Mass Transfer* **2007**, *50*, 4668–4677.
41. Park, J. S.; Choi, C. K.; Kihm, K. D. Temperature Measurement for a Nanoparticle Suspension by Detecting the Brownian Motion Using Optical Serial Sectioning Microscopy. *Meas. Sci. Technol.* **2005**, *16*, 1418–1429.
42. Branson, B. T.; Seif, M. A.; Davidson, J. L.; Lukehart, C. M. Fabrication and Macro/Nanoscale Characterization of Aggregated and Highly De-aggregated Nanodiamond/Polyacrylonitrile Composite Thick Films. *J. Mater. Chem.* **2011**, *21*, 18832–18839.
43. Krüger, A.; Kataoka, F.; Ozawa, M.; Fujino, T.; Suzuki, Y.; Aleksenskii, A. E.; Vul, A. Y.; Osawa, E. Unusually Tight Aggregation in Detonation Nanodiamond: Identification and Disintegration. *Carbon* **2005**, *43*, 1722–1730.